

IN-SITU ORIFICE CALIBRATION FOR REVERSING OSCILLATING FLOW AND IMPROVED PERFORMANCE PREDICTION FOR OSCILLATING WATER COLUMN MODEL TEST EXPERIMENTS

Alan Fleming¹ and Gregor Macfarlane²

¹National Centre for Maritime Engineering and Hydrodynamics, Australian Maritime College,
University of Tasmania, Australia

Performance characterization of oscillating water column (OWC) wave energy converters (WEC) is commonly assessed by conducting physical scale model experiments of OWC models fitted with orifice plates to the air chamber to both; simulate the power take off (PTO), and measure the air flow rate. Generally it is assumed that a single calibration factor can be used for bi-directional air flow measurement, however this paper shows the assumption can be in-accurate and that it is necessary to have separate inflow and outflow calibration factors. This paper presents (i) a novel method for in-situ calibration of an orifice and (ii) a simple algorithm to reduce noise during air flow reversal (low air chamber pressure differential). Application of this technique results in more accurate flow rate prediction and consequently, better prediction of the power absorbed by the power take-off for OWCs.

Keywords: wave energy, oscillating water column, oscillating flow, orifice calibration

1. INTRODUCTION

Model testing of oscillating water column (OWC) wave energy converters at small scale (1:100 – 1:30) presents the issue of only a small amount of power being available (~10 W) for conversion at the power take-off (PTO). Due to scaling effects, system inefficiencies and manufacturing complications the PTO is normally simplified as a simulated PTO [1,2]. The simulated PTO is considered to dissipate the Froude scaled equivalent to the energy equivalently dissipated (converted/wasted) at full scale by the actual PTO [3]. Simulated PTO's are chosen either for their simplicity, or ability to match the pressure/flow characteristics of the design full scale turbine (PTO) [4]. An orifice plate is commonly used to simulate the PTO due to the simplicity in design [2,5–8]. The orifice has a non-linear flow characteristic in that the

differential pressure across the orifice is proportional to the square of the flow through the orifice. Power dissipated by the orifice is proportional to the product of pressure differential across the orifice and the volume flow rate (flux) of air through the orifice [6].

For an OWC, measurement of air volume flux is more difficult using standard flow measurement equipment due the flow continuously changing in both magnitude and direction. Air volume flux may be derived from either:

- a. Water free surface displacement inside the OWC chamber using one or more wave probes [5], or video frames of the free surface displacement [9];
- b. Pressure transducer data using a calibrated orifice [6,7].

There are several arguments why the use of pressure data is preferred to wave probe data for calculation of OWC air volume flux:

- Pressure data is easier to obtain;
- It is not necessary to make assumptions about the nature of the water free surface inside the chamber which ultimately leads to at best greater uncertainty and worst the introduction of error in the calculated value.

However since the air flow oscillates in both magnitude and direction, modelling the relationship between pressure and flow becomes more complicated. In particular; it is known that pressure will vary depending on the physical position of the pressure sensing instrumentation [10–12]. Fig. 1 demonstrates this using data from pressure transducers which monitored pressure inside the air chamber for a model OWC tested in monochromatic waves. The pressure signal is drawn as a solid line with outflow shown in blue and inflow shown in green. Inflow is also inverted as a dashed red line to better enable comparison with the outflow pressure signal. If assuming constant density and using a typical orifice equation (Equation 1) the cumulative sum of the pressure will be proportional to volume flux, to obey with the assumed mass balance for an OWC the slope of the previously mentioned cumulative sum should be zero, since on average volume displaced is also zero.

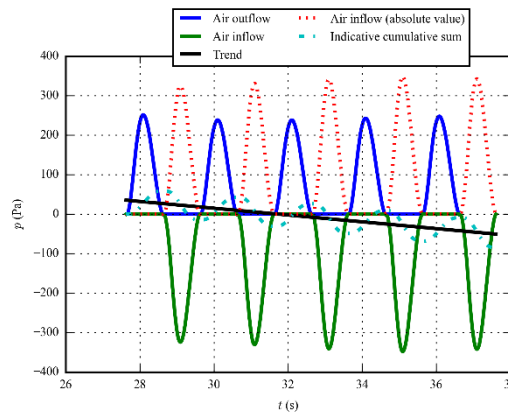


Fig. 1. Typical time series differential air chamber pressure for a model scale oscillating water column.

This paper describes a process to use measure air chamber water surface elevations for in-situ calibration of air flow measurement via determination of air flow coefficients based on air chamber pressure differential measurement. Further; the mass balance error is shown to be reduced by developing flow coefficients separately for both inhalation and exhalation.

2. APPARATUS

The methods presented in this paper consist of two stages; the first being the derivation of flow coefficients using water column displacement data, the second being the estimation of air volume flux application of the flow coefficients. Hence it is not always necessary to complete the first operation if the orifice flow coefficients are already known with a level of certainty. Note that the flow coefficients presented here are strictly only compatible with the orifice used (and perhaps other unknown factors).

Data for this paper is drawn from experiments with a greater ultimate purpose which demonstrates the ‘in situ’ nature of this paper. Experiments were performed on four separate 1:30 scale deep water forward-facing bent-duct OWC models (see Fig. 2 and Table 1 for details). The primary purpose of the experiments was a PIV investigation on the effect of altering OWC geometry [13].

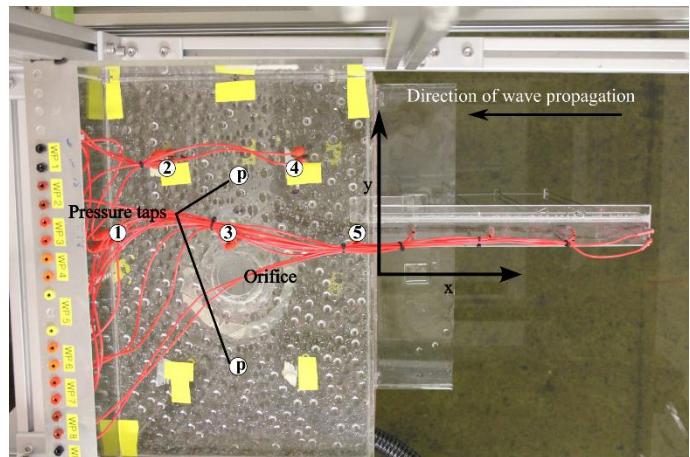
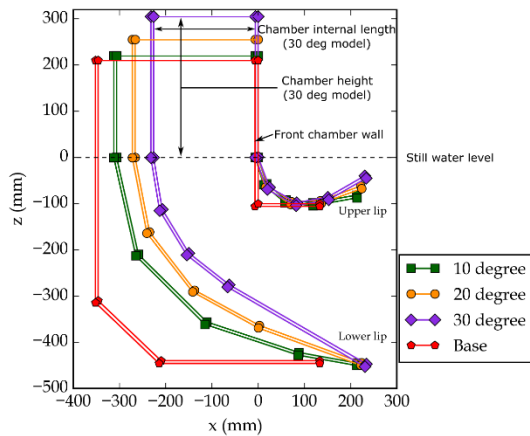


Fig. 2. Left: model geometry profiles and right: Wave probe, pressure tap and orifice plate details [13].

Experiments were conducted in the Australian Maritime College (AMC) towing tank which is 100m long, 3.5m wide and 1.5m deep. A hydraulically driven paddle type wave maker is located at one end of the tank and a passive sloped beach is located at the other end. The models were positioned at the centre of the tank crosswise (one at a time) and approximately 60m from the wave paddle and with the opening of the model facing the incoming waves.

Each OWC was fitted with an array of 5 resistance type wave probes inside the chamber to measure water column heave

(see Table 2 for locations), and a single (external) wave probe adjacent to the front chamber wall. Two Endevco pressure transducers (2 psig Model 8510B-2) monitored chamber differential air pressure in the top plate of the chamber at the centreline half between sidewall and the transverse centreline. A 50.8 mm diameter (D) orifice was included in the top panel of all models ($\delta/D \sim 0.04 < 0.5$ equates to a thin walled orifice as classified by [14] in[8], where $\delta=2$ mm is orifice thickness).

Table 1. Model details

Model	Model width internal (mm)	Chamber length internal (mm)	Damping ratio
10deg	488	300	1/73
20deg	488	260	1/63
30deg	488	220	1/53
Base	506	340	1/85

Table 2. Wave probe locations (x,y) (mm) relative to OWC centreline front face

Model	Probe						
	Incident	Upstream	1	2	3	4	5
10deg	(0,1313)	(1008,-1472)	(-296,50)	(-231,150)	(-156,50)	(-81,150)	(-16,50)
20deg	(0,1313)	(1008,-1472)	(-259,50)	(-206,150)	(-136,50)	(-66,150)	(-13,50)
30deg	(0,1313)	(1008,-1472)	(-214,50)	(-176,150)	(-115,50)	(-60,150)	(-16,50)
Base	(0,1310)	(1008,-1472)	(-335,50)	(-260,150)	(-178,50)	(-90,150)	(-20,50)

Data was acquired at a rate of 1 kHz for the monochromatic wave parameters shown in Table 3 with at least one repeat run and recorded for a duration of approximately 30 s. Where phase averaged data is reported as being used it was processed using the methods described in[15].

Table 3. Wave parameters

Height (m)	Frequency (Hz)
0.04	0.5
0.05	0.5
0.07	0.45, 0.50, 0.55, 0.60, 0.65

3. METHODS

The second stage of the two stage method presented in this paper is the flow-derivation stage. This section describes how to derive the flow rate and how to use this to estimate the orifice flow coefficients. Steady incompressible flow (volume flux) through an orifice is given by [16]

$$Q = C_d A_o \sqrt{2|\Delta p|/\rho} \quad (1)$$

where Q is volumetric flow rate, C_d is discharge coefficient, ρ is density, Δp chamber differential pressure and A_o is the orifice cross-sectional area. Polarity of the pressure differential may be carried outside the radical to indicate flow direction where positive pressure indicates air outflow and negative pressure indicates air inflow (applied in Equation 4).

Rearranging Equation 1 for the flow coefficient:

$$C_d = \frac{Q\sqrt{\rho}}{A_o\sqrt{2|\Delta p|}} \quad (2)$$

Knowledge of the free surface displacement (FSD) is required to derive the flow. The data gathered by the wave probes was used. Volumetric flow was derived using wave probe data for free surface displacement estimation in the OWC chamber. The free surface was assumed to be two-dimensional in cross section. The profile was approximated using a second order polynomial and the velocity was obtained from the derivative of the polynomial. The area between the free-surface and mean water level (polynomial integral) was used to calculate volume flux. The volume flux was treated as periodic and smoothed using that assumption (for more details see[5]).

Using all available phase-averaged volumetric flow and chamber pressure differential data the corresponding orifice flow coefficients were calculated for 100 bins over a wave cycle. The coefficients are plotted against air chamber differential pressure in Fig. 3 (and per Model in Fig. 4). An adjacent incident wave probe was used as the source of the synchronizing signal for phase averaging with a zero up crossing marking the start and finish of the cycle. The vertical grouping of discharge coefficient data points is clearly different between positive and negative differential pressure.

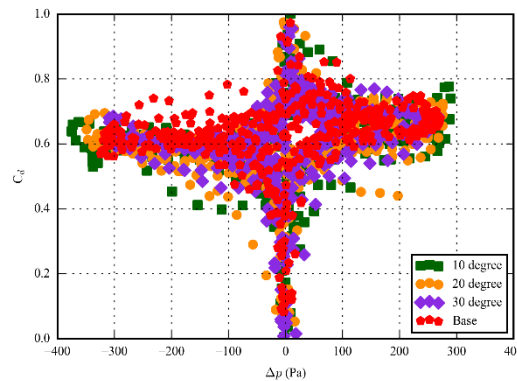
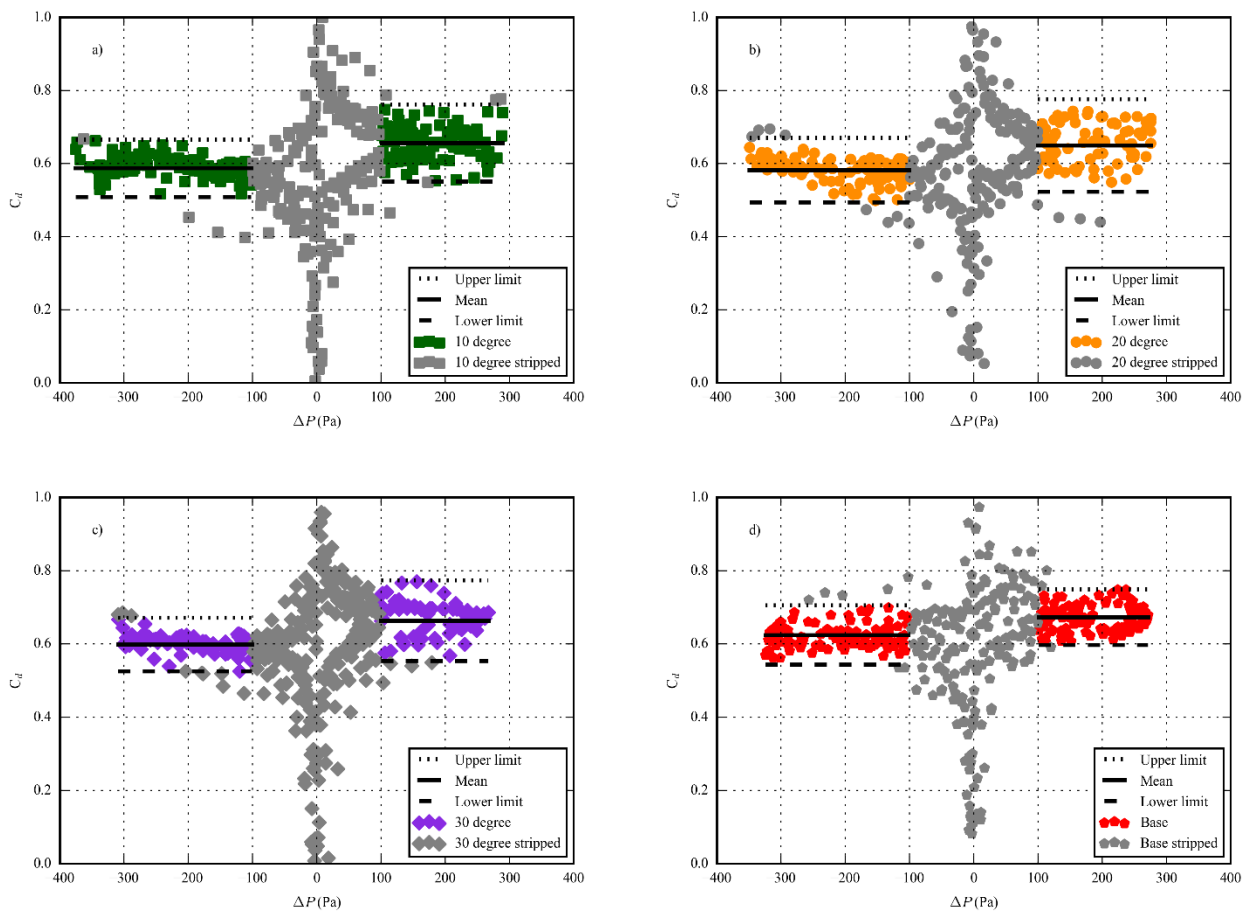


Fig. 3. Discharge coefficient (C_d) verses pressure using phase-averaged wave probe and pressure differential for all available wave conditions and the four different models

112 Separate inflow and outflow coefficients are used to address the pumped volume mass imbalance highlighted in the
 113 introduction (Equation 3). The inflow coefficient was determined per model by taking the average of the coefficients with
 114 corresponding pressures of -100 Pa or less with a pre-filter to discard data outside of two standard deviations of the mean.
 115 Similarly the outflow coefficient had a corresponding pressure of 100 Pa or greater. The corresponding 95 % confidence
 116 interval was derived using two standard deviations of the corresponding sample data. The flow coefficients are presented in
 117 Table 4.
 118



119 **Fig. 4. Visualisation of inflow and outflow discharge coefficient (C_d) verses pressure using phase-averaged wave probe and pressure**
 120 **differential per model for all available data**

121 **Table 4. Flow coefficients**

Model	$C_{d_{in}}$	+ / -	$C_{d_{out}}$	+ / -
Base	0.620	0.008	0.672	0.007
10 deg	0.591	0.012	0.655	0.005
20 deg	0.583	0.011	0.657	0.009
30 deg	0.602	0.009	0.672	0.008
Combined	0.599	0.008	0.664	0.008

Corrected volumetric flow is then calculated using both inflow and outflow coefficients as follows

$$Q = \begin{cases} C_{d_{out}} A_o \sqrt{2|\Delta p|/\rho} & (p > \text{threshold pressure}) \\ -C_{d_{in}} A_o \sqrt{2|\Delta p|/\rho} & (p < -\text{threshold pressure}) \end{cases} \quad (4)$$

where *threshold pressure* = 25 Pa is a limit where data is replaced with cubic spline interpolated values using trend information from the neighbouring data. Spline interpolation is strictly not required, however was useful to remove error caused by a physical hysteresis of the pressure transducer. Spline interpolation can be removed from the mathematical model by setting *threshold pressure* = 0.

Power (energy flux) extracted at the power take-off (PTO) is the product of the volume flux (Q) and pressure differential (Δp) [7]

$$P = \Delta p Q \quad (5)$$

4. RESULTS AND DISCUSSION

Fig. 5 shows a comparison of the chamber volume flux derived using both the wave probe and pressure transducer methods. Flow rates derived from wave probe data exhibit large uncertainty at certain parts over the wave cycle due to the presence of water column slosh being insufficiently approximated by polynomial fitted data of the array of five probes (this uncertainty would be worse for a single probe). The volume flux derived from pressure transducer data is smoother and more likely to be representative of the actual flow but retains an uncertainty comparable to the uncertainty in flow from the wave probe method.

Since pressure and flow are intrinsically linked (pressure differential causes flow), the pressure signal is a more direct source for flow quantification and due to fewer assumptions is arguably more accurate.

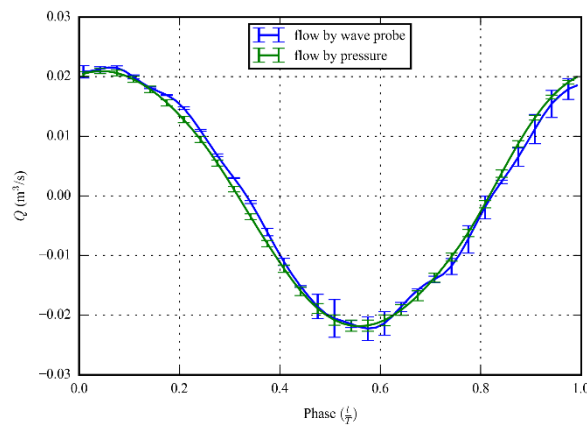


Fig. 5. Phase-averaged volumetric air flow derived from: wave probe data (blue) and pressure transducer data (green). A case taken from Model 10deg (H = 50 mm, T = 2 s).

4.1 Time series air flow

The benefit of using pressure transducer data over wave probe data for air flow quantification becomes even more apparent when applied to time series data. Water sloshing in the chamber and other minor phenomena complicates the process of fitting the free-surface and associated volume flux, with the requirement for additional filtering to prevent massive changes associated with discontinuity affecting the gradient of the volume change between adjacent data points. Furthermore; calculation time increases considerably, though not inhibitably so. The in-situ calibration of the orifice gives greater confidence in the flow coefficients used and further justifies the application of separate inflow and outflow coefficients. Fig. 6 is a plot of a typical time series air flow illustrating the contribution of the coefficients C_{in} , C_{out} with a green and red dashed curve to indicate outflow and inflow respectively as calculated using Equation 4. The black curve is the final accepted flow and the thick blue strokes indicate the parts of the flow which has been interpolated using splines. The correction imposed by the spines is only minor for periodic data, and further is not reliable for polychromatic data. Spline interpolation should therefore not be applied to data corresponding to irregular seas.

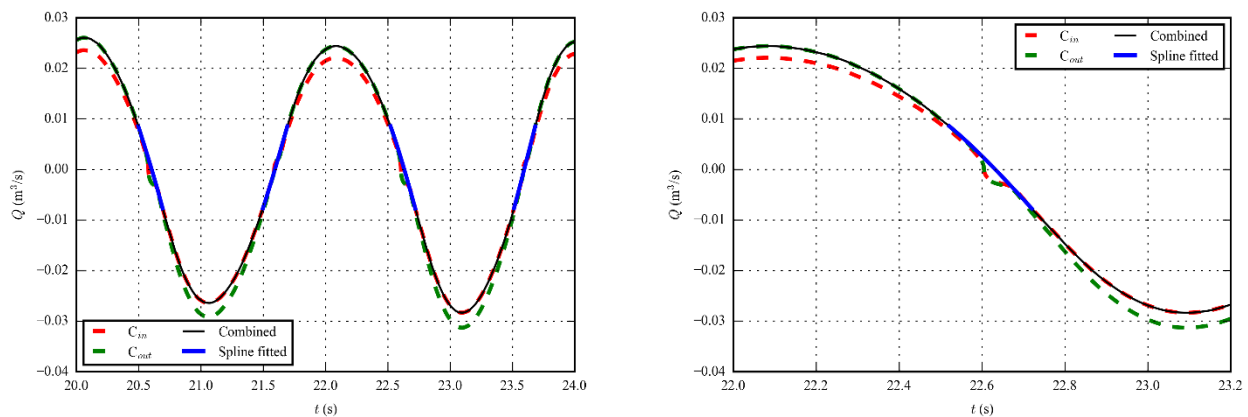


Fig. 6. Typical time series flow through orifice using Equation 4 where the solid line is the combined signals. Left: Several cycles, Right: zoomed in x axis to emphasize hysteresis

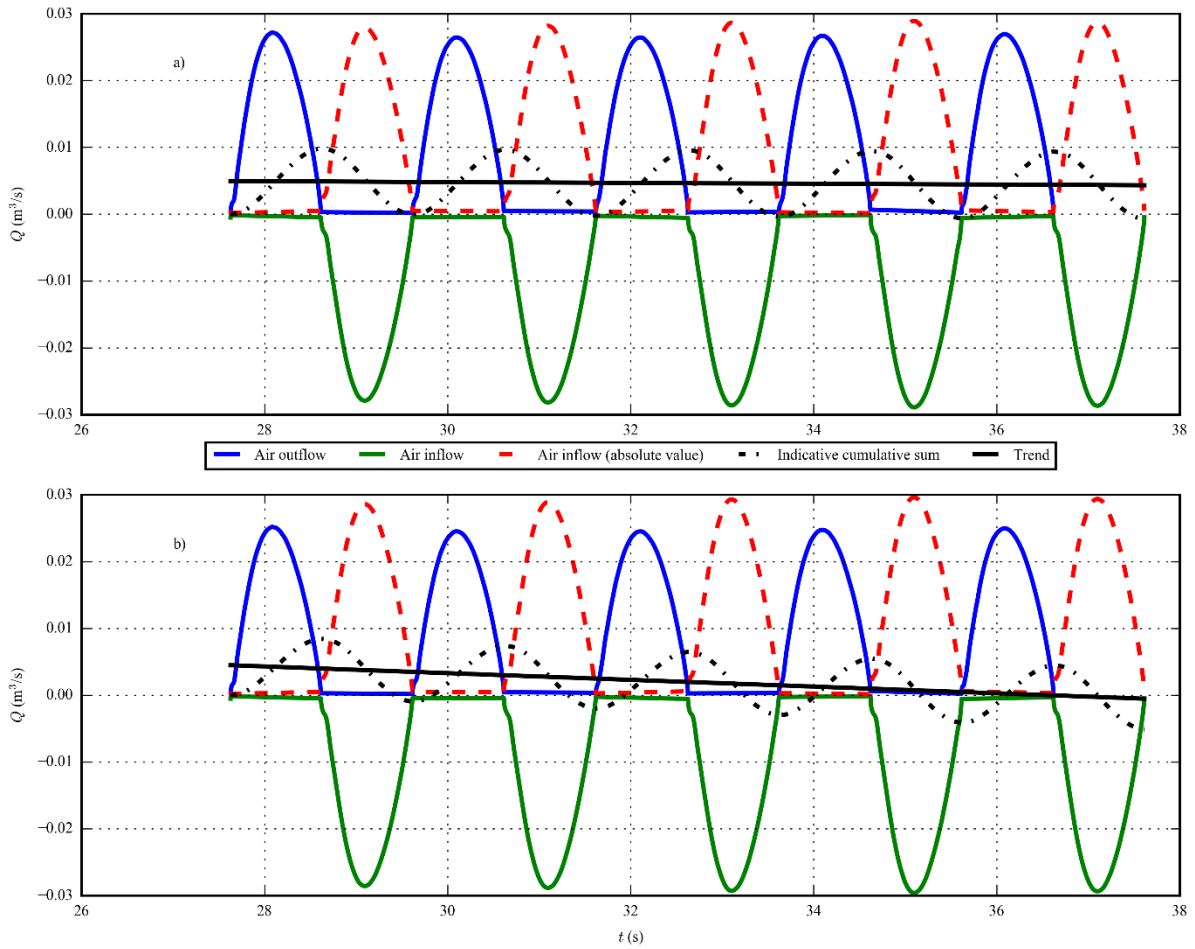
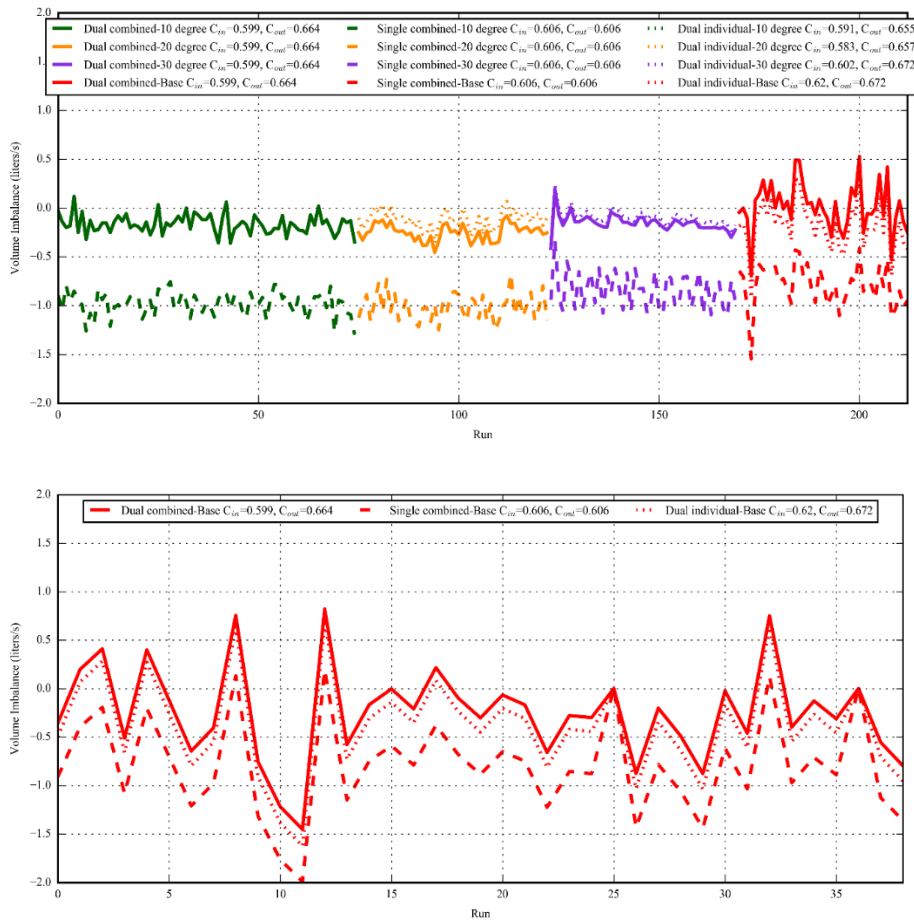


Fig. 7. Typical time series of flow through orifice using a) the new method described; and b) standard flow equation using a single flow coefficient ($C=0.606$) for monochromatic data. Indicative cumulative sum is equivalent to cumulative volume.

The appropriateness of the ratios of the inflow to outflow coefficients is demonstrated in Fig. 7 a) where the slope of the trend of the cumulative sum of the flow (analogous to total volume balance) is close to zero. Fig. 7 b) demonstrates the flow calculated using equal inflow and outflow coefficients ($C_{\text{in}} = C_{\text{out}} = 0.606$) and no spline interpolation. The slope of the indicative cumulative sum is trending downwards indicating that the total volume pumped is also negative which is in error when calculated over multiples of complete wave cycles since the net volume flux is zero.

Fig 8 shows a comparison of volume imbalance using three different types of flow coefficients over the entire monochromatic wave dataset (213 runs with a total run time of 162 minutes) and irregular wave dataset (39 runs with a total run time of 247 minutes) respectively. The solid line represents the recommended method where

171 separate inflow and outflow coefficients are used; average volume imbalance is -0.135 litres/s. The dashed line
 172 represents the standard single flow coefficient method; average volume imbalance is -0.907 litres/s. The dotted
 173 line represents the recommended method, but applied per model rather than the aggregate of the models; total
 174 volume imbalance is -0.143 litres/s. Clearly the dual coefficient method is superior to the single flow coefficient
 175 method. This justifies the use of separate inflow and outflow coefficients and confirms the ratio between them is
 176 approximately correct; however it does not validate the magnitude of the coefficients. An unusual outcome here is
 177 that the individual flow coefficients (dotted line) yield a slightly higher aggregate imbalance compared to the
 178 combined coefficients (solid line), however it is clear in Fig. 8 that both the 20deg and 30deg Models have a
 179 reduced imbalance therefore it is appropriate to adopt the dual flow coefficient method.



180 **Fig. 8. Volume imbalance for entire dataset of 200 + runs using: a) Separate inflow and outflow coefficients (solid line). b)**
 181 **Single flow coefficient (dashed line). c) individual inflow and outflow coefficient for each model (dotted line). Where the top**
 182 **section represents monochromatic wave data and bottom section represent irregular wave data.**

Irregular wave data was only captured for the Base model and is presented as the lower part of Fig. 8. For all methods the magnitude of the volume imbalance is higher, which may be due to the longer periods of low flow. On average the dual coefficient method remains superior with an average imbalance of -0.253 litres/s compared to -0.803 litres/s for the single coefficient method.

4.2 Time series power

Power dissipated across the orifice calculated using Equation 5 using the dual coefficient flow method, and the single coefficient flow method, is illustrated in Fig. 9. The data and times correspond to those in Fig. 6 hence the first and third peaks correspond to outflow and the second and fourth peaks correspond to inflow. The flow corrected method brings the amplitude of the peaks closer together but it is still clear that more energy is dissipated across the orifice during inflow compared to outflow (Fig. 9).

By examining available monochromatic data the ratio of power dissipated across the orifice of outflow to inflow appears to be a function of the devices natural frequency, geometry, the incoming wave frequency and amplitude, and possibly also the water level inside the chamber. On average the ratio is around 0.85 but can vary between 0.7 and 0.95. The significance of this observation may assist the experimentalist in designing the PTO.

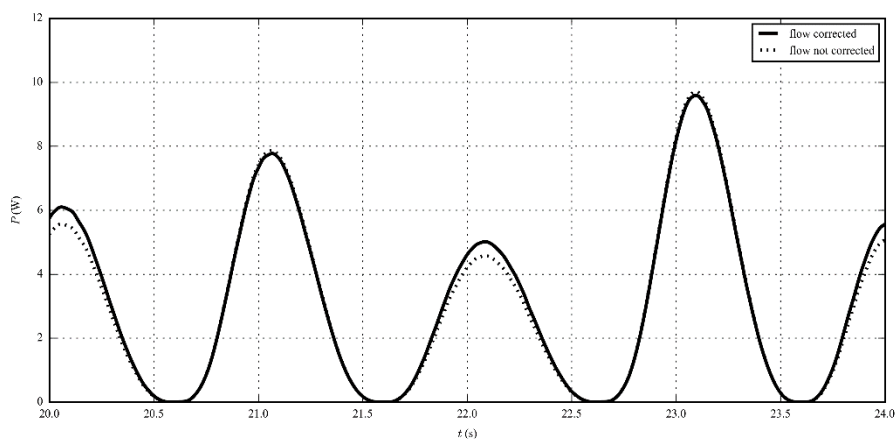


Fig. 9. Typical time series power dissipated across the orifice both corrected flow (solid line) and uncorrected flow (dotted line).

5. CONCLUSIONS

Air volume flux is an important quantity when estimating the performance of OWCs based on indirect measurements during scaled model experiments. It may be calculated from either observed volumetric change, or pressure differential. This paper outlines a novel method for calibrating the second method using the former to yield a prediction relying on fewer assumptions, and ultimately a better approximation of the power absorbed at the simulated power take-off.

For scale model OWC's fitted with an orifice to simulate the power take-off. The use of separate flow coefficients for inflow and outflow yields a better approximation of the actual flow compared to a single flow coefficient. The reduction in error was demonstrated by comparing the mass balance over many wave cycles.

Use of a single flow coefficient in this situation tends to overestimate air inflow and underestimate air outflow with a corresponding impact on power dissipated at the power take-off.

In regular (and near-regular) oscillating air flow conditions; flow data may be spline interpolated for values of low differential pressure (less than 25 Pa in this case). For irregular seas the dual flow coefficient method is equally applicable.

Acknowledgments

This work was supported by the Australian Research Council [grant number LP110200129].

References

- [1] Cruz João, editor. Ocean Wave Energy: Current Status and Future Perspectives. Berlin: Springer Verlag; 2008.
- [2] Falcão AFO, Henriques JCC. Model-prototype similarity of oscillating-water-column wave energy converters. International Journal of Marine Energy 2014;6:18–34. doi:10.1016/j.ijome.2014.05.002.
- [3] Payne GS, Taylor J, Ingram D. Best practice guidelines for tank testing of wave energy converters. The Journal of Ocean Technology 2009;4:38–70.
- [4] Day AH, Babarit A, Fontaine A, He Y-P, Kraskowski M, Murai M, et al. Hydrodynamic modelling of marine renewable energy devices: A state of the art review. Ocean Engineering 2015;108:46–69. doi:10.1016/j.oceaneng.2015.05.036.
- [5] Fleming A, Penesis I, Macfarlane G, Bose N, Denniss T. Energy Balance Analysis for an

Oscillating Water Column Wave Energy Converter. *Ocean Engineering* 2012;54:26–33.
doi:10.1016/j.oceaneng.2012.07.002.

[6] Sarmento AJNA. Wave flume experiments on two-dimensional oscillating water column wave energy devices. *Experiments in Fluids* 1992;12–12:286–92. doi:10.1007/BF00187307.

[7] Sarmento A. Model-test optimization of an OWC wave power plant. *International Journal of Offshore and Polar Engineering* 1993;3:66–72.

[8] He F, Huang Z. Hydrodynamic performance of pile-supported OWC-type structures as breakwaters: An experimental study. *Ocean Engineering* n.d. doi:10.1016/j.oceaneng.2014.04.023.

[9] Mendes AC, Monteiro WML. Performance analysis of a model of OWC energy converter in non-linear waves. *EWTEC 07: 7th European Wave and Tidal Energy Conference*, Porto, Portugal: 2007.

[10] Nielsen J. Effect of turbulence on air-flow measurements behind orifice plates. Langley Field, Va: Langley Memorial Aeronautical Laboratory; 1943.

[11] Narain A, Ajotikar N, Kivisalu MT, Rice AF, Zhao M, Shankar N. Obtaining Time-Varying Pulsatile Gas Flow Rates With the Help of Dynamic Pressure Difference and Other Measurements for an Orifice-Plate Meter. *Journal of Fluids Engineering* 2013;135:041101–041101. doi:10.1115/1.4023195.

[12] Wanzheng A. Energy dissipation characteristics of sharp-edged orifice plate. *Advances in Mechanical Engineering* 2015;7:1687814015595571. doi:10.1177/1687814015595571.

[13] Fleming A, MacFarlane G. Experimental flow field comparison for a series of scale model oscillating water column wave energy converters. *Marine Structures* n.d.;ACCEPTED FOR PUBLICATION.

See:
<https://authors.elsevier.com/tracking/article/details.do?aid=2348&jid=MAST&surname=Fleming>. doi:10.1016/j.marstruc.2016.12.005.

[14] Fossa M, Guglielmini G. Pressure drop and void fraction profiles during horizontal flow through thin and thick orifices. *Experimental Thermal and Fluid Science* 2002;26:513–23. doi:10.1016/S0894-1777(02)00156-5.

[15] Fleming A, Penesis I, Goldsworthy L, Macfarlane G, Bose N, Denniss T. Phase Averaged Flow Analysis in an Oscillating Water Column Wave Energy Converter. *Journal of Offshore Mechanics and Arctic Engineering* 2012;135:021901–[1–9]. doi:10.1115/1.4007076.

[16] Standards Australia. Measurement of Fluid Flow in Closed Conduits. Part 1.1: Pressure Differential Methods-Measurement Using Orifice Plates, Nozzles or Venturi Tubes-Conduits with Diameters from 50 mm to 1200 mm. AS 236011-1993 1993.